J Mater Sci (2008) 43:1880–1884
DOI 10.1007/s10853-007-2418-8

The formation mechanism of titania nanotube arrays in hydrofluoric acid electrolyte

Jing Bai · Baoxue Zhou · Longhai Li · Yanbiao Liu · Qing Zheng · Jiahui Shao · Xinyuan Zhu · Weimin Cai · Junsheng Liao · Lexi Zou

Received: 2 September 2007 / Accepted: 21 December 2007 / Published online: 31 January 2008

Abstract Self-organized and highly ordered titania nanotube arrays (TNAs) were prepared through electrochemical anodic oxidization on a titanium foil in 0.5 wt.% hydrofluoric acid (HF) electrolyte. The current density and morphology images during the formation process of TNAs were studied. Results show that the formation of TNAs includes the following processes. Initially, dense oxide of titania was rapidly formed on the titanium surface, followed by small pore formation. The adjacent small pores were then integrated and become larger pores. At the same time, small tubes were transformed. These small tubes were further integrated into larger tubes until the primary tube formation. Finally, the tubular structure was gradually optimized and eventually developed into the highly ordered TNAs. A model was proposed to explain the formation mechanism of TNAs fabricated on a titanium foil in HF acid electrolyte.

Introduction

It is well known that the properties of functional materials are dependent upon their microstructures. Many kinds of nano-dimensional material like nanowires, nanorods, nanofibers, and nanotubes have been studied extensively [1–3]. Recently, self-organized TNAs on a titanium (Ti) substrate fabricated by potentiostatic anodic oxidation were first reported by Grimes and his colleagues [4]. Their special nanoarchitecture offers a large internal surface area without a concomitant decrease in geometric and structural order [5, 6]. The precisely oriented structure makes them excellent electron percolation pathways for vectorial charge transfer between interfaces and offers them improved properties for applications in the fields of solar cell, photocatalysis, water photolysis, hydrogen sensors, and others [7–24].

Parameters, such as electrolyte composition, anodization voltage and time, influence the growth of titania nanotube arrays during the anodization. Grimes and co-workers [25] observed the appearance of pores and voids on the surface of titanium foil in the formation process of nanotube. They believed that the tube structure was a result from deepening and expansion of the small pores. Schmuki and co-workers [26] found that the low acidity at the pore bottom help to etch the pore into a tubular structure. However, the detailed processes of how the small pore transforms into a large pore and eventually a tubular structure are not clear.

In this study, TNAs were prepared by anodic oxidization in a 0.5 wt.% HF acid electrolyte at 10 and 20 V, respectively. The current density and morphology images during the preparation were studied. On the basis of the above observation, a model was proposed to explain the possible formation mechanism of TNAs fabricated on a titanium foil in HF acid electrolyte.

Experiments

Titanium foils (0.1 mm thick) with a purity of 99.99% (Kurumi works, Japan) were used to prepare the TNAs.

J. Bai · B. Zhou (✉) · L. Li · Y. Liu · Q. Zheng · J. Shao · X. Zhu · W. Cai
School of Environmental Science and Engineering, Shanghai Jiao Tong University, Shanghai 200240, People's Republic of China
e-mail: zhoubaoxue@sjtu.edu.cn

J. Liao · L. Zou
China Academy of Engineering Physics, Mianyang 621900, People's Republic of China

The foils were cleaned with macro 90 (surfactant) in an ultrasonic bath, followed by rinsing in deionized water and finally drying in air. The concentration of the HF acid was 0.5 wt.%. The nanotubes were grown by potentiostatic anodization at either 20 or 10 V using a platinum cathode. A direct-current power with a programmable function was used to control the current and voltage. The structure and morphology of the TNAs were characterized by a field emission scanning electron microscope (FESEM, FEI-Sirion200). SEM cross-sectional observations were carried out on mechanically bent samples.

Results and discussion

Figure 1 gives variation of the anodization current (a, c) and thickness (b, d) with time at anodization potential of 20 and 10 V for 1 h in 0.5 wt.% HF acid electrolyte. The change of current density with time at two anodization voltages appears to follow a similar trend, which can be summarized in three stages: a descent stage, a gradually ascent stage and a steady stage. In the first stage, the current density decreased rapidly. This change can be attributed to the formation of dense oxide layer, which increased the resistance immensely. In the second stage, the current density began to increase and keep growth due to the effect of the gradually enhanced electric-field-assistant dissolution of titania, which decreased the surface resistance of titanium foil. In the third stage, the current density keeps relatively stable value since it reaches the maximum dissolution rate of titania at the nanotube bottom. It can be seen from Fig. 1a, c that the current density at 20 V is nearly twice as high as that at 10 V. Moreover, it takes longer time (about 500 s) to reach the stable value.

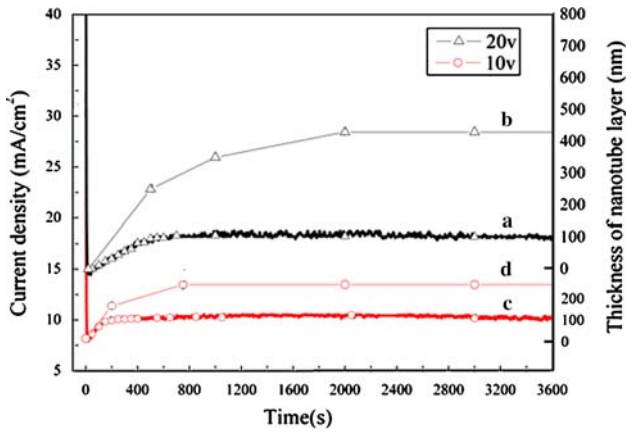

Fig. 1 Variation of the anodization current (**a** and **c**) and thickness (**b** and **d**) with time at anodization potential of 20 and 10 V for 1 h in 0.5 wt.% HF acid electrolyte

The above processes can be ascribed to the interaction of the following two chemical reactions equations:

$$Ti + 2H_2O - 4e \rightarrow TiO_2 + 4H^+ \quad (1)$$

$$TiO_2 + 6F^- + 4H^+ \rightarrow [TiF_6]^{2-} + 2H_2O \quad (2)$$

Figure 1b, d shows that the variation of thickness with time corresponding to each variation of the anodization current with time. The increasing current density leads to a rapid increment of thickness and the thickness keeps a relatively fixed value when the current density maintains relative stable in the third stage. The self-organized and highly ordered TNAs can be obtained for a long time anodization. It can be seen from Fig. 2 that the morphology of the as-fabricated TNAs is influenced evidently by anodization voltage. The length and diameter of TNAs are approximately 430 and 100 nm, respectively, at 20 V, and only 250 and 30 nm at 10 V. This means that the structural parameters of TNAs can be fixed for a certain anodization voltage.

Figure 3 shows the FESEM images of the samples anodized at 20 V for different duration (10, 30, 60, 200, 800, and 1,800 s) in 0.5 wt.% HF acid electrolyte. At 10 s, the surface was covered with a dense oxide film of titania at the initial stage (Fig. 3a). At 30 s (Fig. 3b), the original oxide film was clearly dissolved and formed a continuous wormlike layer. This can be attributed to localized dissolution of the oxide by HF [25]. With further anodization at 60 s (Fig. 3c), most of the original oxide film layer was removed and replaced by a film comprised of small pores with diameter ranging from 8 to 15 nm. The inset in Fig. 3c shows a large pore was formed by the integration of some smaller pores. The following image after 200 s shows a process of small tubes turning into a larger one, meanwhile, the discrete tubular structures with uneven diameter ranging from approximately 20–100 nm can also be observed (Fig. 3d). This shows that the tubular structure is transformed from the large pore, which derives from integration of the earlier small pores. At 800 s, the primary nanotube arrays with the diameter about 100 nm were formed (Fig. 3e). After an anodization period of 1,800 s, highly ordered TNAs approximately 100 nm in diameter was fully developed (Fig. 3f).

On the basis of the above experiments, it can be concluded that the appearance of a large pore is caused by an integration of initial small pores and the tubular structure derives from the further integration of the large pores and small nanotubes. The highly ordered TNAs are developed from primary tube arrays. A model was proposed and a further explanation on the formation mechanism of TNAs was given.

In the initial stage, the current density decreased sharply because of the formation of dense oxide (Fig. 4a). The

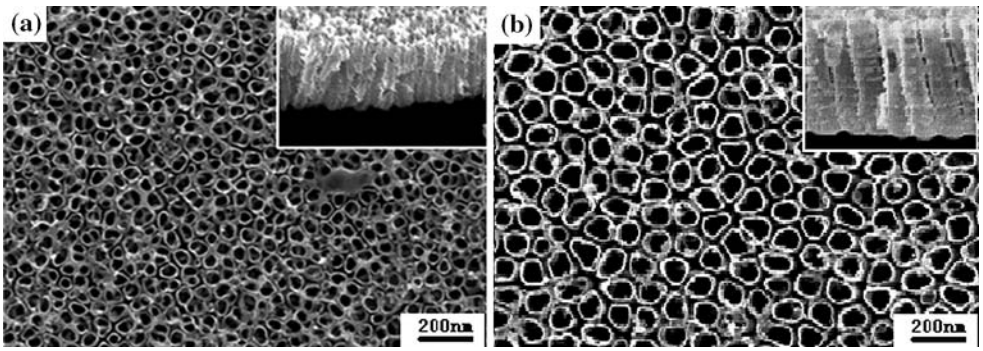

Fig. 2 SEM images of the top view and cross-section of TiO_2 nanotube arrays formed at 10 V for 1 h (**a**) and 20 V for 1 h (**b**) in a 0.5 wt.% HF acid electrolyte

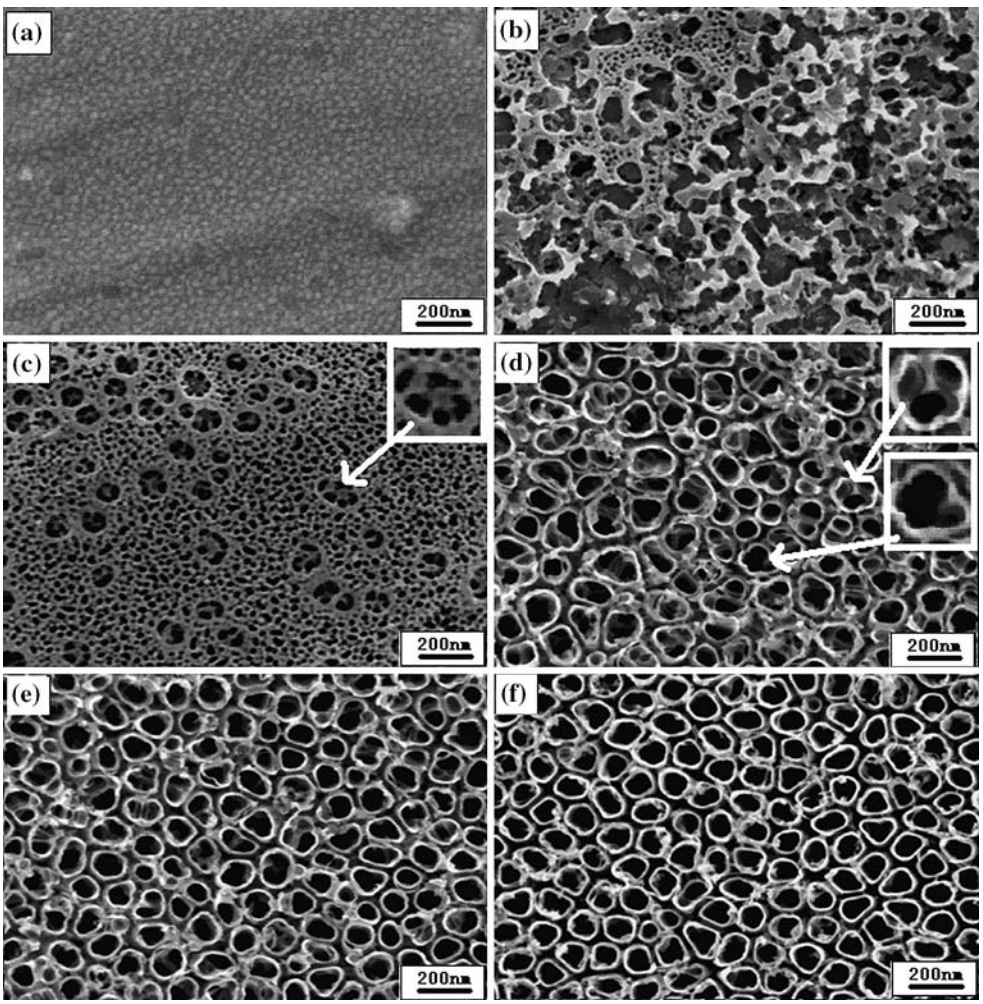

Fig. 3 SEM top-views (**a**–**f**) of titania nanotube arrays formed at 20 V in 0.5 wt.% HF acid electrolyte at different anodization time (**a**) 10 s, (**b**) 30 s, (**c**) 60 s, (**d**) 200 s, (**e**) 800 s, and (**f**) 1,800 s

initial dense oxide was then dissolved immediately by the HF acid (Eq. 2), and many small pores were formed on the surface of the newly-generated barrier layer (Fig. 4b). Because the initial small pores are very narrow, while a mass of H^+ ions are generated at the bottom of the pore where Ti came out of the metal and dissolved in the solution (Eqs. 1 and 2), and the concentration of HF acid inside the pores increases rapidly. High concentration of HF acid makes the wall of pores dissolve until the adjacent walls disappear. At the same time, the integration by small

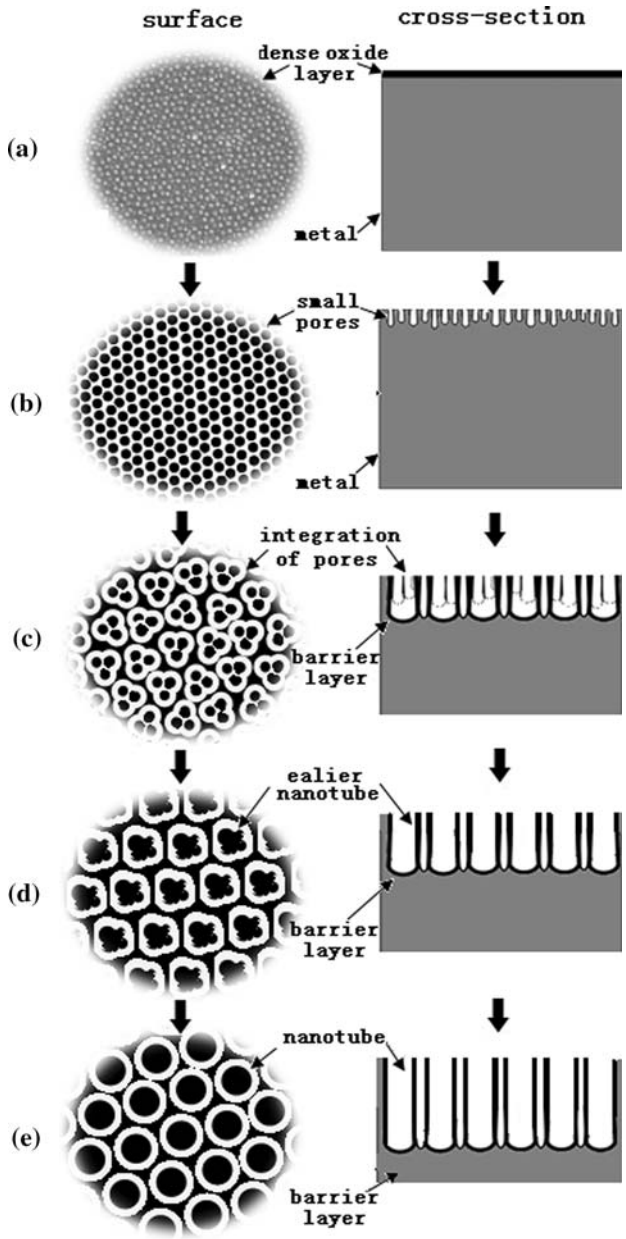

Fig. 4 Schematic diagram of the evolution of straight nanotubes at a constant anodization voltage, as follows: (**a**) dense oxide layer formation, (**b**) pore formation and deepening, (**c**) integration of some adjacent small pores into a big one, (**d**) earlier nanotube arrays formation, and (**e**) perfect nanotube arrays formation

pores results in the appearance of lager pores. Simultaneously, the enhanced electric-field-assisted dissolution at the pore bottom leads to a deepening of the pore and the voids start forming (Fig. 4c). The overall result is the formation of the earlier tubular structure (Fig. 4d).

The electric-field-assisted dissolution reaction results in acidity varied from the pore bottom to the pore mouth, where lead to different local chemical etch rates between them. Because the rate at the bottom is higher than that at the top, the length of tubes gradually increases until they become equal. With increasing anodization time, the tubular structure is gradually optimized, and the length and diameter of TNAs keep relatively stable value. The full-developed TNAs are developed finally (Fig. 4e).

Conclusion

Titania nanotube arrays were fabricated by electrochemical anodic oxidation on a pure titanium foil in a 0.5 wt.% HF acid electrolyte. The analysis of surface morphology, variation of the anodization current and thickness with time during the anodization demonstrates that the formation process of TNAs includes following stages, the formation of dense oxide, the integration of pores, the further transformation of a small tube into a larger tube, and the formation of a fully developed nanotube. At last, a schematic diagram to describe the mechanism of nanotubes formation was proposed.

Acknowledgements This work was supported by the National Nature Science Foundation of China (No. 20677039), Science and Technology Commission of Shanghai Municipality (No. 05nm05004) and the Program of New Century Excellent Talents in University (No. NCET-04-0406). Thanks for support of FE-SEM lab in Instrumental Analysis Center of SJTU.

References

1. Miao Z, Xu D, Ouyang J, Guo G, Zhao X, Tang Y (2002) Nano Lett 2:717
2. Limmer SJ, Chou TP, Cao GZ (2004) J Mater Sci 39:895
3. Kasuga T, Hiramatsu M, Hoson A, Sekino T, Niihara K (1998) Langmuir 14:3160
4. Gong D, Grimes CA, Varghese OK, Hu W, Singh RS, Chen Z, Dickey EC (2001) J Mater Res 16:3331
5. Maggie P, Karthik S, Sorachon Y, Haripriya EP, Oomman KV, Mor GK, Thomas AL, Adriana F, Grimes CA (2006) J Phys Chem B 110:16179
6. Mor GK, Oomman KV, Maggie P, Karthik S, Grimes CA (2006) Sol Energ Mater Sol C 90:2011
7. Vitiello RP, Macak JM, Ghicov A, Tsuchiya H, Dick LFP, Schmuki P (2006) Electrochem Commun 8:544
8. Chuanmin R, Maggie P, Oomman KV, Grimes CA (2005) Sol Energ Mater Sol C 90:1283
9. Karthik S, Kong CT, Mor GK, Grimes CA (2006) J Phys D: Appl Phys 39:2361
10. Xie YB (2005) Electrochim Acta 51:3399
11. Lai YK, Sun L, Chen YC, Zhuang HF, Lin CJ, Chin JW (2006) J Electrochem Soc 153:123
12. Quan X, Yang SG, Ruan XL, Zhao HM (2005) Environ Sci Technol 39:3770
13. Xie Y (2006) Nanotechnology 17:3340
14. Mor GK, Oomman KV, Maggie P, Grimes CA (2003) Sensor Lett 1:42
15. Oomman KV, Maggie P, Karthik S, Mor GK, Grimes CA (2005) J Nanosci Nanotechnol 5:1158

16. Mor GK, Shankar K, Paulose M, Varghese OK, Grimes CA (2006) Nano Lett 6:215
17. Jong HP, Kim SW, Bard AJ (2006) Nano Lett 6:24
18. Macak JM, Hiroaki T, Andrej G, Schmuki P (2005) Electrochem Commun 7:1133
19. Maggie P, Karthik S, Oomman KV, Mor GK, Grimes CA (2006) J Phys D: Appl Phys 39:2498
20. Wang H, Yip CT, Cheung KY, Djurisic AB, Xie MH, Leung YH, Chan WK (2006) Appl Phys Lett 89
21. Andrei G, Macak JM, Hiroaki T, Julia K, Volker H, Lothar F, Schmuki P (2006) Nano Lett 6:1080
22. Andrei G, Macak JM, Hiroaki T, Julia K, Volker H, Sebastian K, Schmuki P (2006) Chem Phys Lett 419:426
23. Zhao JL, Wang XH, Sun TY, Li LT (2005) Nanotechnology 16:2450
24. Wang M, Guo DJ, Li HL (2005) J Solid Stage Chem 178:1996
25. Mor GK, Oomman KV, Maggie P, Niloy M, Grimes CA (2003) J Mater Res 18:2588
26. Macak JM, Hiroaki T, Schmuki P (2005) Angew Chem Int Ed 44:2100